Article

Discovery Medicine 2026; 38(208): 1537–1550
https://doi.org/10.24976/Discov.Med.202638208.120

Beyond Prolonged Fever: Synergistic Value of LDH and IL-6 for Early Stratification of Severe Mycoplasma Pneumoniae Pneumonia in Children

Ruonan Zhang[1], Chaoqun Zhou[1], Jinghua Li[1], Dike Huang[1,*]

[1]Department of Pediatrics, The Affiliated Yangming Hospital of Ningbo University, 315400 Ningbo, Zhejiang, China
*Correspondence: Htt060901@163.com (Dike Huang)
Submitted: 21 January 2026 Revised: 24 March 2026 Accepted: 3 April 2026 Published: 20 May 2026

Background: The incidence of severe Mycoplasma pneumoniae pneumonia (SMPP) in children has markedly increased in the post-COVID-19 era. Current diagnosis approaches often rely on persistent fever, which may delay early identification. This study aims to evaluate the synergistic value of Lactate Dehydrogenase (LDH) and Interleukin-6 (IL-6) for early stratification.
Methods: We retrospectively analyzed clinical data from 210 hospitalized children with Mycoplasma pneumoniae pneumonia (MPP; 120 severe and 90 non-severe). Independent risk factors were identified using multivariate logistic regression to build a dynamic nomogram. To validate the model's early warning capability and exclude circularity, a specific subgroup analysis was performed on patients admitted in the early phase of illness (fever duration <7 days).
Results: LDH, IL-6, and pre-admission fever duration were independent predictors. The combined nomogram outperformed single biomarkers with an Area Under the Curve (AUC) of 0.827. Crucially, in the early-phase subgroup, both IL-6 and LDH remained significantly elevated in SMPP cases ($p < 0.05$), proving that pathological signals precede the clinical threshold for severity. The study revealed a "two-axis" mechanism whereby IL-6 quantified systemic inflammation, while LDH reflected local tissue hypoxia (e.g., atelectasis), distinct from the systemic response. Decision Curve Analysis further confirmed the model's clinical utility.
Conclusion: This study proposes a dual-pathology stratification model where IL-6 reflects cytokine storm and LDH indicates tissue injury. The nomogram reliably identifies high-risk children in the early illness phase, facilitating intervention before persistent fever develops.

Keywords: Mycoplasma pneumoniae pneumonia; lactate dehydrogenase; interleukin-6; nomogram; early stratification; pediatric

Introduction

Mycoplasma pneumoniae (MP) is a predominant pathogen underlying community-acquired pneumonia (CAP) in children, accounting for approximately 10% to 40% of pediatric CAP cases worldwide [1,2]. While Mycoplasma pneumoniae pneumonia (MPP) has traditionally been regarded as a self-limiting disease, its epidemiology has shifted significantly in the post-COVID-19 era [3–5]. Recent surveillance data indicate a resurgence of MP infections with an alarming escalation in the incidence of severe MPP (SMPP) and refractory MPP (RMPP) [6,7]. Unlike mild cases, SMPP can rapidly progress to life-threatening complications, including necrotizing pneumonia, pulmonary embolism, and bronchiolitis obliterans, often leaving permanent functional sequelae [8,9]. Consequently, the "window of opportunity" for effective intervention, such as the timely administration of corticosteroids or therapeutic bronchoscopy, is limited [10,11].

Current clinical guidelines primarily define severity based on persistent fever, deterioration of radiological findings, or hypoxia [11]. Reliance on these macroscopic indicators, however, presents a fundamental limitation, as they often manifest only after significant immunopathological damage has already occurred [12,13]. Pulmonary consolidation and atelectasis, hallmarks of SMPP, are radiological consequences of established inflammation and mucus plugging rather than early warning signals [14,15]. This temporal lag necessitates the identification of sensitive, dynamic biological markers capable of reflecting disease progression at the molecular and cellular levels before irreversible structural injury ensues.

The pathogenesis of SMPP involves a complex interplay between direct pathogen-induced cytotoxicity and an excessive host immune response, often termed a "cytokine storm" [16,17]. Interleukin-6 (IL-6), a pleiotropic pro-inflammatory cytokine, serves as a pivotal upstream regulator in this cascade, triggering the synthesis of acute-phase reactants and regulating the systemic inflammatory response [17,18]. Parallel to systemic inflammation, lo-

cal tissue hypoxia and endothelial injury are critical drivers of severity. Lactate dehydrogenase (LDH), an intracellular enzyme released upon cell membrane disruption, has emerged as a robust predictor of RMPP and mucus plug formation [19,20]. While elevated LDH is traditionally interpreted solely as an inflammatory marker, recent evidence suggests it more specifically quantifies cellular necrosis and hypoxic burden distinct from the cytokine signaling reflected by IL-6 [21,22].

Despite the extensive study of these biomarkers individually, few investigations have systematically analyzed their complementary roles in the early stratification of SMPP. Most predictive models treat LDH and IL-6 as parallel inflammatory indices, potentially overlooking their synergistic value in capturing distinct pathological dimensions of systemic immune intensity versus end-organ cytotoxicity. This study aims to bridge this gap by analyzing the clinical data of hospitalized children with MPP. We sought to elucidate the differential diagnostic value of LDH and IL-6 and construct a multivariate nomogram. However, a major limitation in current predictive models is the heavy reliance on fever duration as a predictor, which often overlaps with the diagnostic criteria for SMPP, leading to potential circular reasoning. It remains unclear whether biomarkers like LDH and IL-6 can stratify risk before fever duration achieves the severity thresholds. Therefore, this study not only constructs a multivariate nomogram but also specifically validates the differential diagnostic value of these biomarkers in the early phase of the disease (fever <7 days) to ensure actual predictive utility. By integrating these biomarkers with clinical features, we intend to provide a precise, quantifiable tool for the early identification of high-risk patients, thereby guiding rational therapeutic decision-making.

Methods

Study Design and Population

We collected clinical data from children hospitalized with Mycoplasma pneumoniae pneumonia (MPP) between June 2023 and December 2025. The inclusion criteria were age <14 years; diagnosis of MPP based on clinical presentation, radiological findings, and positive M. pneumoniae serology (immunoglobulin M, IgM; SERODIA-MYCO II particle agglutination assay, Fujirebio Inc., Tokyo, Japan) or polymerase chain reaction (PCR; ABI 7500 Real-Time PCR System Applied Biosystems, Foster City, CA, USA); and complete medical records. The exclusion criteria were co-infection with other pathogens (bacteria, viruses, or fungi); history of chronic lung diseases, immunodeficiency, or congenital heart disease; and missing key laboratory data (specifically LDH or IL-6 levels).

The study protocol was approved by the Ethics Committee of The Affiliated Yangming Hospital of Ningbo University (approval number: 2026-01-003). The Ethics Committee waived the requirement for individual informed consent, given the retrospective nature of the study and the use of de-identified, pre-existing clinical data with no direct patient contact.

Grouping Criteria

Patients were divided into a Severe MPP (SMPP) group and a Non-Severe MPP (NSMPP) group according to the Guidelines for Diagnosis and Treatment of Mycoplasma Pneumoniae Pneumonia in Children (2023 Edition) [11] and the Guidelines for the Management of Community-Acquired Pneumonia in Children [23–25]. SMPP was defined by the presence of at least one of the following: persistent high fever (>39 °C) for ≥ 7 days or fever duration ≥ 10 days; rapid progression of radiological findings (infiltration increasing $>50\%$ within 24–48 hours); presence of complications such as lung consolidation, atelectasis, necrotizing pneumonia, or lung abscess; and resting hypoxia (peripheral oxygen saturation, SpO2 $<93\%$).

Data Collection and Preprocessing

Clinical data were extracted from electronic medical records, including demographic characteristics (age, gender, weight), clinical symptoms (fever duration, length of hospital stay [LOS]), laboratory findings, and imaging features. To ensure the early predictive value of the model and avoid circular reasoning with the grouping criteria, "Fever Duration" was strictly defined as the number of days of fever before hospital admission (or study enrollment). Total duration of fever during the entire course of the disease was recorded for descriptive comparison but was excluded from the predictive model construction. Laboratory indicators also included Lactate Dehydrogenase (LDH), Interleukin-6 (IL-6), C-reactive protein (CRP), and D-dimer. All blood samples were collected within 24 hours of admission. LDH was measured using a lactate-to-pyruvate kinetic rate assay on a Beckman Coulter AU5800 automated analyzer (Beckman Coulter, Inc., Brea, CA, USA), with an institutional reference interval of 120–300 U/L for the pediatric age group. IL-6 was quantified by electrochemiluminescence immunoassay (ECLIA) on a Roche Cobas e801 platform (Roche Diagnostics GmbH, Mannheim, Germany) using the Elecsys IL-6 assay kit (Cat. No. 05109442190, Roche Diagnostics GmbH, Mannheim, Germany), with a reference interval of <10 pg/mL. CRP was measured by immunoturbidimetric assay on a Beckman Coulter AU5800 automated analyzer (Beckman Coulter, Inc., Brea, CA, USA). D-dimer was measured by immunoturbidimetric assay on a Sysmex CS-5100 automated coagulation analyzer (Sysmex Corporation, Kobe, Japan).

Numerical Conversion: All laboratory values were stored as exact numeric values in the database. No inequality-symbol entries (e.g., "<0.5", ">220") were present in the final dataset.

Table 1. Baseline demographic and clinical characteristics of children with MPP.

Variable	Level	Overall	Non-Severe	Severe	Statistic (Z/χ^2)	p	Test
n		210	90	120			
Age (median [IQR])		6.88 [4.75, 8.73]	6.96 [4.50, 8.48]	6.83 [5.12, 9.10]	Z = –0.889	0.374	nonnorm
Gender (%)	Female	118 (56.2)	54 (60.0)	64 (53.3)	χ^2 = 0.929 (df = 1)	0.335	Chi-square
	Male	92 (43.8)	36 (40.0)	56 (46.7)			
Weight (median [IQR])		22.25 [17.60, 30.08]	21.90 [17.60, 28.03]	22.40 [17.80, 31.30]	Z = –0.620	0.536	nonnorm
Fever_Days (median [IQR])		6.00 [5.00, 8.00]	5.00 [4.00, 6.00]	8.00 [7.00, 9.00]	Z = –10.196	<0.001	nonnorm
LOS (median [IQR])		5.00 [4.00, 7.00]	4.00 [4.00, 6.00]	6.00 [4.75, 8.00]	Z = –4.868	<0.001	nonnorm
LDH (median [IQR])		274.50 [245.25, 321.00]	261.00 [236.25, 294.25]	292.00 [258.00, 343.50]	Z = –3.849	<0.001	nonnorm
IL-6 (median [IQR])		18.15 [11.23, 27.18]	12.64 [7.79, 17.57]	25.18 [15.89, 33.81]	Z = –7.616	<0.001	nonnorm
CRP (median [IQR])		14.05 [6.38, 28.38]	10.50 [4.93, 21.01]	17.35 [7.80, 34.68]	Z = –3.524	<0.001	nonnorm
D_Dimer (median [IQR])		571.50 [388.75, 899.50]	450.50 [334.00, 585.50]	724.50 [512.50, 1168.50]	Z = –5.839	<0.001	nonnorm
Is_Multilobe (%)	No	83 (39.5)	52 (57.8)	31 (25.8)	χ^2 = 21.956 (df = 1)	<0.001	Chi-square
	Yes	127 (60.5)	38 (42.2)	89 (74.2)			
Has_Atelectasis (%)	No	201 (95.7)	90 (100.0)	111 (92.5)	Fisher's exact	0.011	exact
	Yes	9 (4.3)	0 (0.0)	9 (7.5)			
Has_Effusion (%)	No	148 (70.5)	90 (100.0)	58 (48.3)	Fisher's exact	<0.001	exact
	Yes	62 (29.5)	0 (0.0)	62 (51.7)			
Age (%)	<6 years	71 (33.8%)	33 (36.7%)	38 (31.7%)	χ^2 = 0.575 (df = 1)	0.448	Chi-square
	≥6 years	139 (66.2%)	57 (63.3%)	82 (68.3%)			

Data are presented as median [interquartile range, IQR] for non-normally distributed continuous variables or as number (percentage, %) for categorical variables. Z-statistics are derived from the Mann-Whitney U test (normal approximation) for continuous variables. χ^2 statistics are from Pearson chi-square tests without Yates' continuity correction. Fisher's exact test was applied for Has_Atelectasis and Has_Effusion due to zero-cell counts. Abbreviations: MPP, Mycoplasma pneumoniae pneumonia; LOS, length of hospital stay; LDH, Lactate Dehydrogenase; IL-6, Interleukin-6; CRP, C-reactive protein.

Feature Extraction: Imaging phenotypes and complications were extracted from textual radiological reports using keyword matching. "Multi-lobe involvement" was defined by the presence of terms such as "multi-lobe" or "bilateral" in the report. Specific complications such as "Atelectasis" and "Pleural Effusion" were encoded as binary variables (Yes/No).

Age Standardization: Age recorded in "Years + Months" format was converted into decimal years for continuous variable analysis.

Statistical Analysis

All statistical analyses and graphics were performed using R software (version 4.4.2; R Foundation for Statistical Computing, Vienna, Austria) with the tidyverse (v2.0.0), rms (v6.8-1), pROC (v1.18.5), and ggpubr (v0.6.0) packages.

Descriptive Statistics: Continuous variables were first tested for normality using the Shapiro-Wilk test. Non-normally distributed data (e.g., LDH, IL-6, CRP, LOS) were presented as median [interquartile range, IQR] and compared between groups using the Mann-Whitney U test. Categorical variables were expressed as frequencies (percentages) and compared using the Chi-square test or Fisher's exact test.

Subgroup Analysis for Early Validation: To evaluate the early predictive utility of the biomarkers and exclude potential circular reasoning arising from the severity criterion (fever duration before admission >7 days), a subgroup analysis was performed. We restricted the dataset to patients admitted in the early phase of the disease (fever duration before admission <7 days). The Mann-Whitney U test was used to compare LDH and IL-6 levels between the Severe and Non-Severe groups within this sub-cohort.

Correlation Analysis: The Spearman rank correlation coefficient was calculated to evaluate the associations between biomarkers (LDH, IL-6) and clinical burden indicators (CRP, D-dimer, fever duration, and LOS).

Model Construction: Univariate logistic regression analysis was performed to screen for potential risk factors. Variables with $p < 0.05$ in the univariate analysis were included in the multivariate logistic regression model to identify independent risk factors for SMPP. Results were reported as Odds Ratios (ORs) with 95% Confidence Intervals (CIs).

Nomogram Development: Based on the identified independent predictors, a diagnostic nomogram was constructed using the rms package to estimate the probability of SMPP.

Model Validation: The discriminative ability of the model was assessed using the Receiver Operating Characteristic (ROC) curve and the Area Under the Curve (AUC). Internal validation was performed using bootstrap resampling (B = 1000 iterations). In each iteration, a bootstrap sample was drawn with replacement from the original dataset, the model was re-fitted, and its predictions were applied back to the original sample to estimate optimism-corrected performance. The calibration of the model was assessed using the resultant bootstrap-corrected calibration curve. This approach provides an optimism-corrected estimate of model performance and guards against overfitting, serving as a rigorous form of internal cross-validation appropriate for the current sample size. Decision Curve Analysis (DCA) was employed to assess the clinical utility of the nomogram.

A two-tailed p-value < 0.05 was considered statistically significant.

Results

Baseline Characteristics and Group Differences

A total of 210 children with Mycoplasma Pneumoniae Pneumonia (MPP) were included in the final analysis after data cleaning and exclusion of cases with missing key biomarkers. The cohort was divided into the SMPP group (n = 120) and the NSMPP group (n = 90) based on clinical severity.

As illustrated in Fig. 1, there were statistically significant differences in inflammatory biomarkers between the two groups. The median serum LDH levels were significantly higher in the Severe group compared to the Non-Severe group (292.00 vs. 261.00 U/L, $p < 0.001$). Similarly, IL-6 levels were markedly elevated in the Severe group (25.18 vs. 12.64 pg/mL, $p < 0.0001$). Additionally, as summarized in Table 1, patients in the Severe group exhibited a longer duration of fever (8.00 vs. 5.00 days) and a longer length of hospital stay (LOS) compared to the Non-Severe group ($p < 0.001$). Age stratification revealed that 71 (33.8%) patients were aged <6 years and 139 (66.2%) were aged ≥ 6 years. The proportion of younger children (<6 years) did not differ significantly between the SMPP and NSMPP groups (36.7% vs. 31.7%, $p = 0.448$), suggesting that age was not a major determinant of disease severity in this cohort.

Biomarker Levels in Early-Phase Patients (Fever Duration <7 Days)

To verify whether LDH and IL-6 serve as early warning signals rather than mere consequences of prolonged disease, we analyzed a subgroup of 114 patients admitted with a fever duration of less than 7 days. Among them, 24 progressed to SMPP, while 90 remained non-severe.

Crucially, even in this early-phase cohort, both biomarkers remained significantly elevated in the Severe group. The median IL-6 levels were significantly higher in the Severe group compared to the Non-Severe group (Mann-Whitney U test, W = 563, $p < 0.001$). Similarly, LDH levels were significantly elevated in the Severe group (W = 743, $p = 0.019$). These findings, illustrated in Fig. 2, demonstrate that the immunological divergence precedes

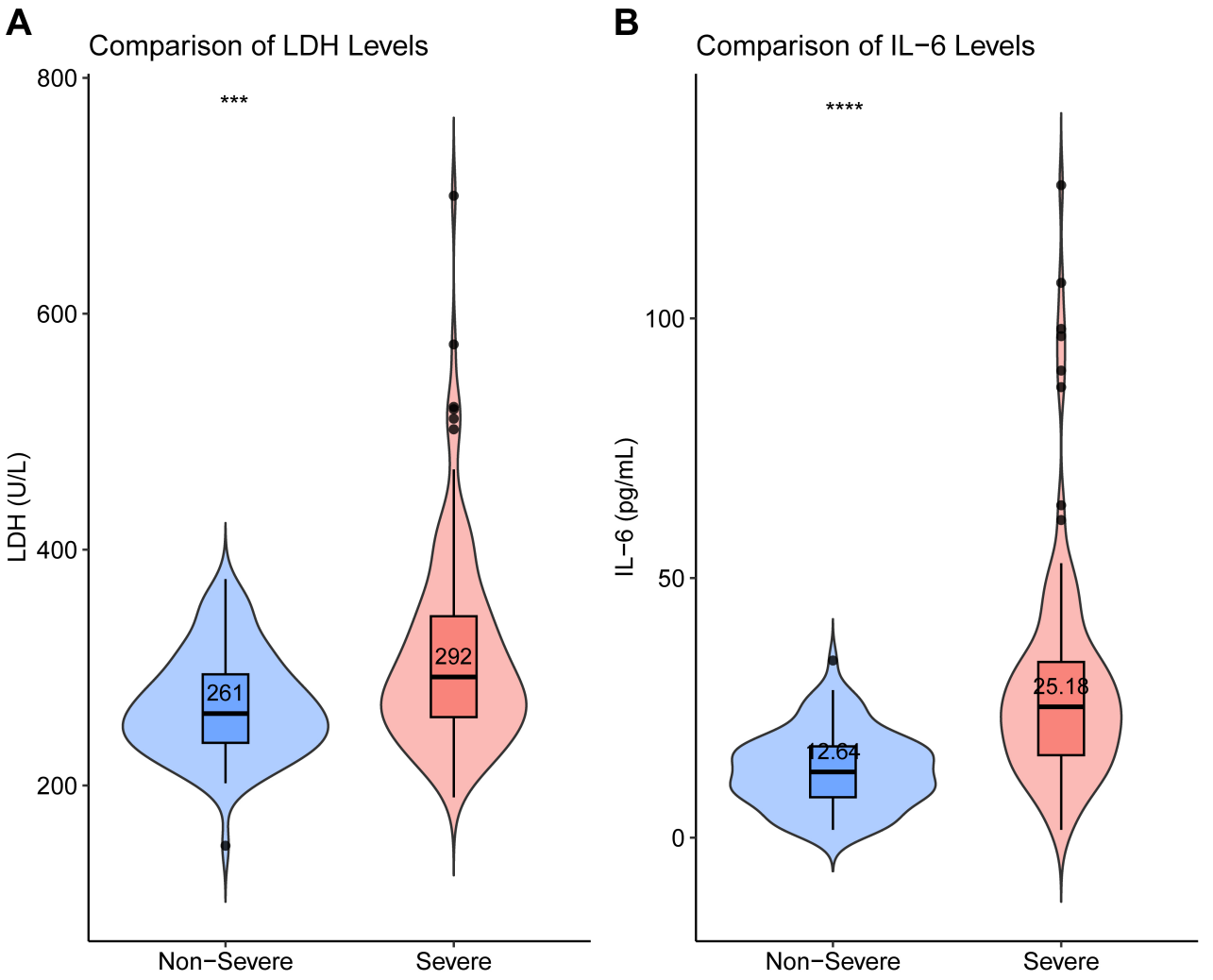

Fig. 1. Comparison of serum biomarker levels between the Non-Severe and Severe MPP groups. Violin plots combined with box plots showing the distribution of (A) Lactate Dehydrogenase (LDH) and (B) Interleukin-6 (IL-6) levels. The width of the violin represents the probability density of the data, and the box plot displays the median and interquartile range (IQR). Statistical significance was determined using the Mann-Whitney U test. Abbreviations: MPP, Mycoplasma pneumoniae pneumonia; LDH, lactate dehydrogenase; IL-6, interleukin-6. Asterisks indicate statistical significance: ***$p < 0.001$, ****$p < 0.0001$.

the clinical severity threshold defined by fever duration. In this early-phase subgroup, 24 of 114 patients (21.1%) were ultimately classified as SMPP, while 90 (78.9%) remained non-severe. This distribution reflects two convergent factors. The SMPP diagnostic criteria (e.g., persistent fever $\geq$7 days, radiological progression, or complications such as atelectasis) inherently require a period of disease evolution to manifest, so patients captured within the first week of fever are less likely to have yet met the formal severity threshold at the time of biomarker sampling. Another, the composition of this subgroup differs from the overall cohort (SMPP 120/210, 57.1%) because our overall enrollment intentionally included a substantial proportion of severe cases to ensure sufficient statistical power for the primary analysis. Whereas the early-phase subgroup was defined purely by fever duration and therefore approximates the natural early-presentation population more closely. Despite this class imbalance, the Mann-Whitney U test is robust to unequal group sizes, and the significant elevations of both IL-6 ($p < 0.001$) and LDH ($p = 0.019$) in the 24 SMPP cases indicate effect sizes large enough to be detected even in a smaller severe subgroup, supporting the biological robustness rather than a statistical artifact.

Screening for Risk Factors of SMPP

Univariate logistic regression analysis indicated that the duration of fever (OR = 2.737, 95% CI: 2.111–3.727, $p < 0.001$), LDH levels (OR = 1.011, 95% CI: 1.006–1.017, $p < 0.001$), IL-6 levels (OR = 1.133, 95% CI: 1.092–1.181, $p < 0.001$), CRP ($p = 0.040$), and D-dimer ($p = 0.021$) were significantly associated with the occurrence of SMPP. Age and gender showed no statistically significant correlation with disease severity ($p > 0.05$).

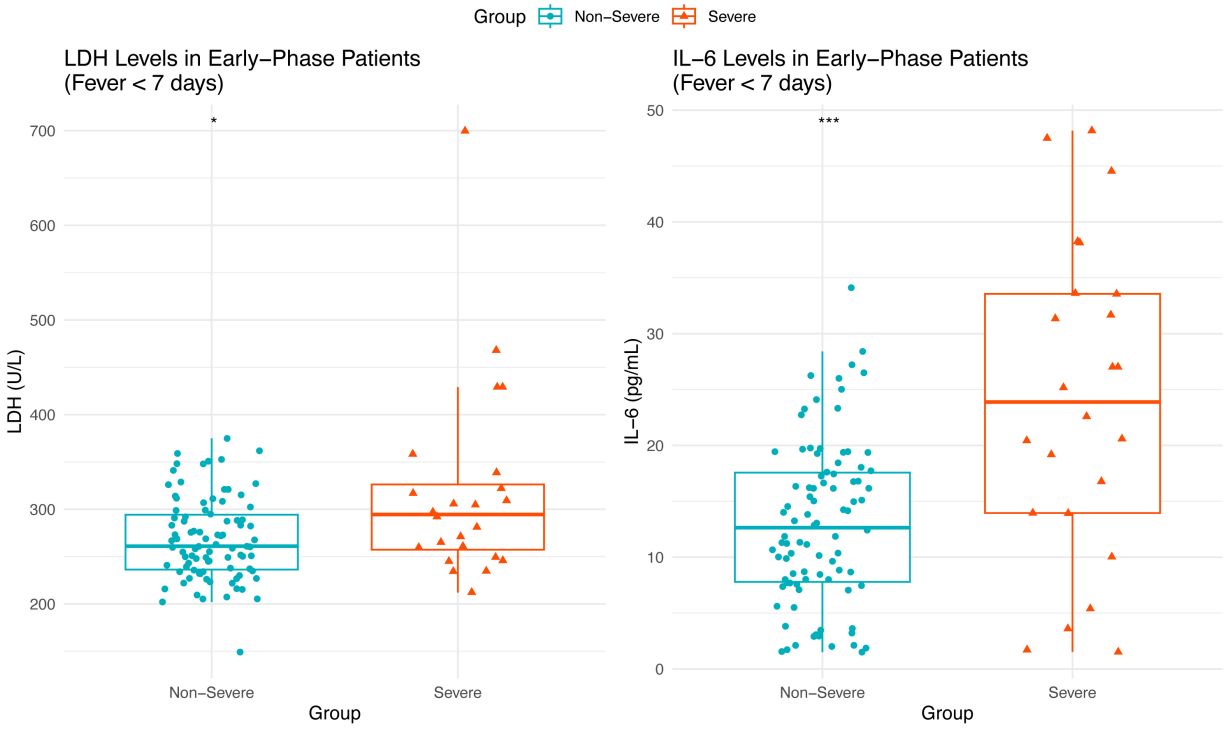

Fig. 2. Comparison of serum biomarker levels in the early-phase subgroup (fever duration <7 days). Boxplots showing the distribution of Lactate Dehydrogenase (LDH) and Interleukin-6 (IL-6) levels in patients admitted within the first week of fever. Despite the exclusion of patients with prolonged fever, the Severe group (n = 24) exhibited significantly higher levels of both biomarkers compared to the Non-Severe group (n = 90). The boxes represent the median and interquartile range (IQR). Statistical analysis was performed using the Wilcoxon rank-sum test with continuity correction. *$p < 0.05$, ***$p < 0.001$.

To identify independent predictors, variables with $p < 0.05$ in univariate analysis, namely fever duration, LDH, IL-6, CRP and D-dimer, were included in the multivariate logistic regression analysis. The results demonstrated that LDH (OR = 1.009, 95% CI: 1.001–1.018, $p = 0.044$), IL-6 (OR = 1.087, 95% CI: 1.038–1.147, $p = 0.001$), and duration of fever (OR = 2.252, 95% CI: 1.725–3.096, $p < 0.001$) were independent risk factors for SMPP. Although CRP ($p = 0.040$) and D-dimer ($p = 0.021$) were statistically significant in univariate analysis and were therefore included in the multivariate model, neither remained independently significant after mutual adjustment for the other covariates (CRP: adjusted OR 0.999, 95% CI 0.983–1.012, $p = 0.935$; D-dimer: adjusted OR 1.000009, 95% CI 0.999775–1.000336, $p = 0.943$). This attenuation likely reflects collinearity among CRP, D-dimer, and the more proximal inflammatory mediator IL-6, which accounts for much of their variance in the multivariate context. Consequently, only LDH, IL-6, and pre-admission fever duration were regarded as independent predictors for nomogram construction. The detailed results of the logistic regression analysis are presented in Table 2.

Diagnostic Value of LDH and IL-6

ROC curve analysis was performed to evaluate the individual and combined predictive value of LDH and IL-6 for the early identification of SMPP (Fig. 3). LDH alone achieved an Area Under the Curve (AUC) of 0.655, with an optimal cut-off value of 291.50 U/L (sensitivity 0.508, specificity 0.733). IL-6 alone yielded a higher AUC of 0.807 (cut-off value 19.84 pg/mL, sensitivity 0.666, specificity 0.877). The Combined Model (LDH + IL-6) demonstrated the highest overall diagnostic accuracy with an AUC of 0.827. Notably, while the increment in AUC was modest compared to IL-6 alone, the combination substantially improved the specificity to 0.827 (sensitivity 0.625, cut-off value 0.69). This indicates that integrating LDH with IL-6 enhances the model's ability to exclude non-severe cases, thereby providing superior utility for clinical stratification.

Construction and Validation of the Nomogram

Based on the multivariate logistic regression analysis, LDH, IL-6, and pre-admission fever duration were identified as independent risk factors for SMPP. These three significant predictors were incorporated into the construction of a diagnostic Nomogram (Fig. 4A). By locating the patient's values on the respective variable axes of LDH level, IL-6 level, and days of fever, and summing the corre-

Table 2. Univariate and multivariate logistic regression analysis of risk factors associated with severe MPP.

Variable	Univariate	*P*_Uni	Multivariate	*P*_Multi
Age	1.045 (0.947–1.154)	0.384	-	-
Gender (male vs. female)	1.313 (0.756–2.292)	0.336	-	-
Fever_Days	2.737 (2.111–3.727)	<0.001	2.252 (1.725–3.096)	<0.001
LDH	1.011 (1.006–1.017)	<0.001	1.009 (1.001–1.018)	0.044
IL6	1.133 (1.092–1.181)	<0.001	1.087 (1.038–1.147)	0.001
CRP	1.015 (1.002–1.031)	0.040	0.999 (0.983–1.012)	0.935
D_Dimer	1.000632 (1.000186–1.001234)	0.021	1.000009 (0.999775–1.000336)	0.943

Univariate analysis identifies factors significantly associated with disease severity. Multivariate analysis determines independent risk factors after adjusting for confounding variables. The confidence interval for D-dimer is reported to six decimal places to ensure the lower bound is distinguishable from the null value of 1.000. Odds Ratios (ORs) are presented with 95% Confidence Intervals (CIs).

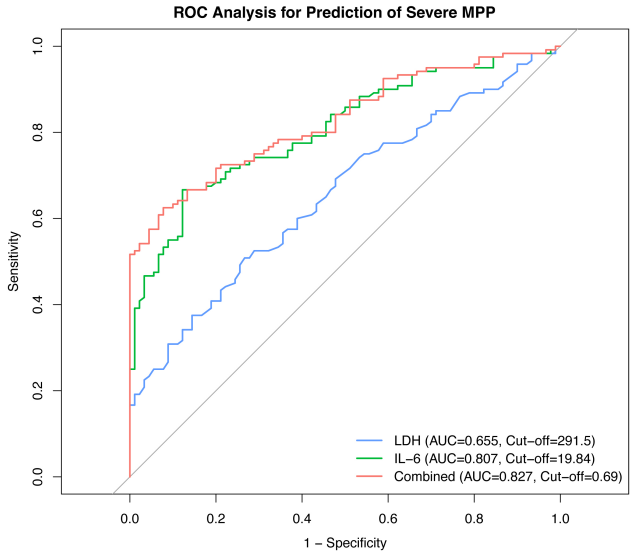

Fig. 3. Receiver Operating Characteristic (ROC) curve analysis for the prediction of severe MPP. The graph illustrates the diagnostic performance of LDH alone (blue line), IL-6 alone (green line), and the Combined Model (red line) constructed using logistic regression. The Area Under the Curve (AUC) values indicate that the combined model provides superior predictive accuracy compared to single biomarkers.

sponding points, clinicians can quantitatively estimate the individual probability of developing SMPP. The model's performance was further assessed via the calibration curve (Fig. 4B), which demonstrated excellent agreement between predicted probabilities and observed outcomes. The curve showed a low Mean Absolute Error (MAE) of 0.061 (based on B = 1000 bootstrap resamples, Mean squared error = 0.00494, 0.9 Quantile of absolute error = 0.115), indicating the high reliability and reproducibility of the nomogram estimates in this cohort. While fever duration is a well-established clinical predictor, our analysis highlights that the addition of serum biomarkers (LDH and IL-6) provides critical immunological and pathological insights beyond those captured by clinical symptoms alone.

Decision Curve Analysis (DCA)

Decision Curve Analysis (DCA) was performed to assess the clinical utility of the predictive model in guiding intervention strategies (Fig. 5). The analysis demonstrated that the Combined Nomogram Model (integrating LDH, IL-6, and pre-admission fever duration) yielded the highest net benefit across a broad range of threshold probabilities (approx. 10% to 75%). Notably, the combined model consistently outperformed both the "treat-all" and "treat-none" strategies, as well as the single-biomarker models (LDH alone or IL-6 alone). These findings suggest that the developed nomogram to stratify patients offers superior clinical value compared to individual biomarkers, effectively optimizing the trade-off between identifying high-risk SMPP cases and minimizing unnecessary medical interventions.

Association With Imaging Phenotypes: LDH Reflects Tissue Hypoxia Rather Than Spatial Extent

To elucidate the specific pathological dimension represented by LDH, we analyzed its correlation with distinct radiological phenotypes (Fig. 6).

We observed a clinically significant dissociation between LDH levels and the spatial extent of infiltration. As shown in Fig. 6A, patients with multi-lobe or bilateral involvement did not exhibit statistically higher median LDH levels compared to those with single-lobe involvement (281 vs. 270 U/L, $p = 0.210$). This suggests that systemic LDH elevation does not merely scale with the radiological surface area of inflammation. In contrast, LDH levels were robustly sensitive to signs of airway obstruction and tissue hypoxia. Patients complicated with pulmonary atelectasis had significantly elevated LDH levels compared to those without (median 403 vs. 273 U/L; $p = 0.019$; Fig. 6B).

This finding strongly implies that LDH release in SMPP is driven primarily by local cellular necrosis and hypoxic-ischemic injury (processes intensified by mucus plugging and atelectasis) rather than by the generalized inflammatory load, which is better captured by fever duration or CRP.

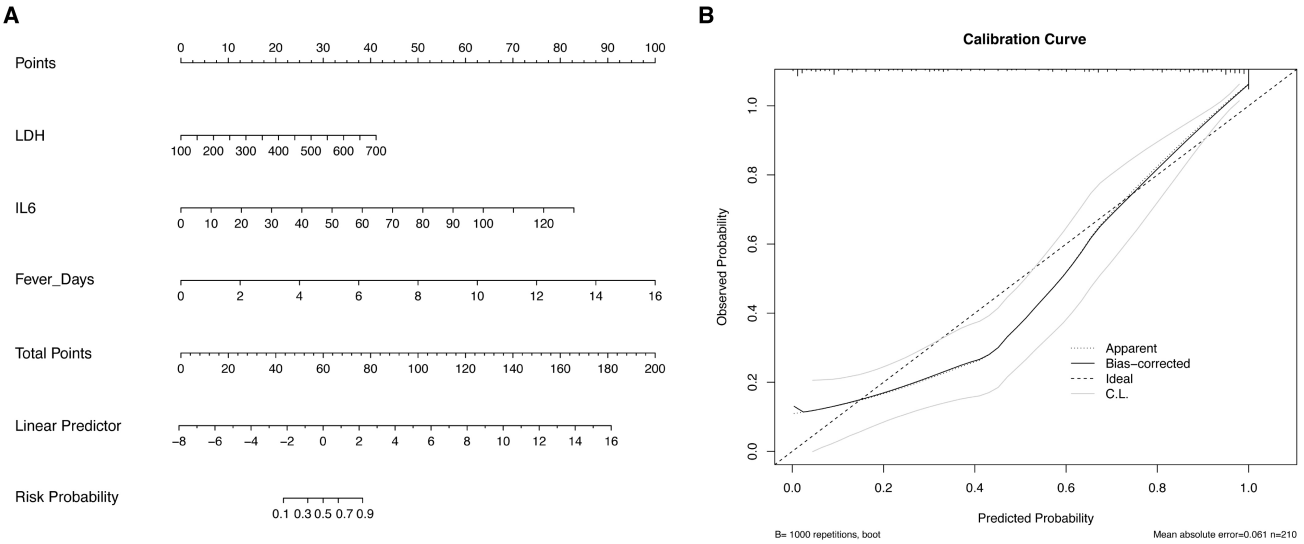

Fig. 4. Diagnostic nomogram for predicting the probability of SMPP and the calibration curve. (A) A predictive tool constructed based on the multivariate logistic regression model. To use the nomogram, locate the patient's values for each variable on the corresponding axes, draw a vertical line upwards to the "Points" scale to determine the score for each variable, sum the points, and locate the total on the "Total Points" scale. Draw a vertical line downwards to the "Risk Probability" axis to obtain the estimated probability of SMPP. The units of LDH and IL-6 are U/L and pg/mL, respectively. (B) Calibration curve of the Nomogram. The x-axis represents the predicted probability of SMPP calculated by the nomogram, and the y-axis represents the actual observed probability. The diagonal dotted line represents ideal prediction (perfect calibration). The solid line represents the performance of the nomogram based on bootstrap resampling (B = 1000), indicating good agreement between the predicted probability and observed probability.

We further examined the association between IL-6 levels and the same imaging phenotypes to determine whether it paralleled or diverged from the LDH pattern. As shown in Fig. 7, in contrast to LDH, IL-6 levels were significantly elevated in patients with multi-lobe or bilateral involvement compared to those with single-lobe disease (median [IQR]: 20.43 [12.62, 31.01] vs. 16.15 [9.58, 23.30] pg/mL; $p = 0.013$), but did not differ significantly between patients with and without atelectasis (median 27.02 vs. 17.73 pg/mL; $p = 0.096$). This dissociation represents the inverse of the LDH pattern and provides direct evidence for the "two-axis" hypothesis: IL-6 scales with the spatial extent of pulmonary inflammation, reflecting systemic immune activation, whereas LDH is selectively elevated in the presence of airway obstruction and tissue hypoxia, independent of the overall radiological burden.

Correlation Analysis

Spearman correlation analysis (Table 3) was performed to evaluate the associations between biomarkers, inflammatory burden, and clinical outcomes.

LDH levels demonstrated moderate but significant positive correlations with D-dimer (r = 0.395, $p < 0.001$), duration of fever (r = 0.273, $p < 0.001$), and length of hospital stay (LOS) (r = 0.271, $p < 0.001$). Crucially, however, no statistically significant correlation was observed between LDH or CRP levels (r = 0.071, $p = 0.309$). This lack of correlation suggests that LDH elevation in SMPP follows a distinct pathological trajectory, likely reflecting tissue hypoxia and necrosis, that is largely independent of the CRP-mediated systemic inflammatory cascade.

In contrast, IL-6 levels exhibited broad and significant positive correlations with all examined parameters. Notably, IL-6 showed the strongest correlation with the duration of fever (r = 0.522, $p < 0.001$) and CRP (r = 0.412, $p < 0.001$), while also correlating with D-dimer (r = 0.389) and LOS (r = 0.356).

Overall, these findings indicate a functional divergence: while both markers correlate with disease severity, IL-6 aligns more closely with the intensity of the systemic inflammatory response (e.g., fever and CRP), whereas LDH serves as an independent indicator of cellular injury and coagulopathy (D-dimer), largely independent of the acute-phase response pathway.

Discussion

This retrospective cohort study successfully established and validated a diagnostic nomogram for the early prediction of Severe Mycoplasma Pneumoniae Pneumonia (SMPP) in children. By integrating serum Lactate Dehydrogenase (LDH), Interleukin-6 (IL-6), and pre-admission fever duration, our multivariate model demonstrated superior predictive performance (AUC = 0.827) compared to single-biomarker assessments. Beyond standard diagnostic metrics, the Decision Curve Analysis (DCA) confirmed the model's clinical utility.

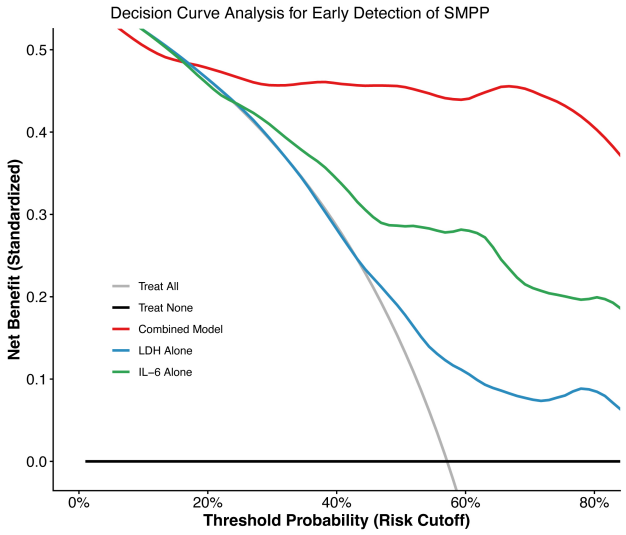

Fig. 5. Decision Curve Analysis (DCA) for the early prediction of severe Mycoplasma pneumoniae pneumonia (SMPP). The y-axis measures the net benefit, and the x-axis represents the threshold probability. The red solid line represents the combined nomogram model (integrating LDH, IL-6, and pre-admission fever duration). The blue solid line and green solid line represent the models based on LDH alone and IL-6 alone, respectively. The gray solid line represents the assumption that all patients have SMPP (Treat All), while the black solid line represents the assumption that no patients have SMPP (Treat None). The combined model exhibits the highest net benefit across a wide range of threshold probabilities, indicating superior clinical utility compared to single biomarkers.

Table 3. Spearman correlation analysis between serum biomarkers and clinical parameters.

Indicator	Correlated_With	r_value	*p*_value
LDH	Fever_Days	0.273	<0.001
LDH	LOS	0.271	<0.001
LDH	CRP	0.071	0.309
LDH	D_Dimer	0.395	<0.001
IL6	Fever_Days	0.522	<0.001
IL6	LOS	0.356	<0.001
IL6	CRP	0.412	<0.001
IL6	D_Dimer	0.389	<0.001

Evaluation of the linear relationship between key biomarkers (LDH, IL-6) and clinical outcome measures (fever duration, hospital stay), as well as other inflammatory markers. Abbreviations: r, Spearman correlation coefficient.

A critical strength of our study is the rigorous validation of biomarkers in the early-phase subgroup (fever <7 days). A common criticism of SMPP prediction models is the circularity introduced when prolonged fever serves as both a predictor and a grouping criterion. Our findings effectively address this limitation. The persistence of statistically significant elevations in IL-6 and LDH among severe cases in the early-phase subgroup indicates that the intense inflammatory response and tissue hypoxia begin well before the clinical criteria for SMPP are met. This implies that our nomogram does not merely "diagnose" established severity based on time accumulation but "predicts" progression based on pathological divergence. This temporal precedence is vital for clinicians, enabling the identification of high-risk phenotypes within the first week of illness, thereby opening a valid window for preemptive intervention (e.g., corticosteroids or bronchoscopy).

A central contribution of our study is the proposal of a "two-axis" pathological model for stratifying SMPP severity, highlighting the critical divergence between IL-6 and LDH. The first axis represents Systemic Immune Intensity, principally characterized by IL-6. As a pivotal initiator of the cytokine storm, IL-6 triggers the downstream release of acute-phase reactants [26]. Our data revealed a strong positive correlation between IL-6, CRP (r = 0.412), and fever duration (r = 0.522). This confirms that IL-6 quantifies the magnitude of the host's systemic inflammatory response, answering the question of how aggressively the immune system reacts [27]. Unlike CRP, which lags behind acute inflammatory signaling, IL-6 rises earlier, serving as a sensitive marker for the early-stage detection of the immune response [28,29]. Since the elevation of LDH in our cohort appears to signal a distinct pathological dimension: cellular cytotoxicity and vascular endothelial injury [30], the second axis represents End-Organ Hypoxic Burden and Cytotoxicity, distinctively captured by LDH. Crucially, our analysis showed that LDH had no significant correlation with CRP (p = 0.309) and was not driven merely by the radiological extent of infiltration (multi-lobe involvement). Instead, LDH was robustly elevated in patients with atelectasis. This pattern supports the hypothesis that LDH operates on a separate axis, likely reflecting cellular necrosis caused by local tissue hypoxia and mucus plugging [31,32], though direct histological validation of this mechanism was beyond the scope of the present study. LDH specifically quantifies the resultant cellular injury and vascular damage [33,34], providing an estimate of the structural damage present in the lung tissue.

This "two-axis" distinction elucidates the mechanism of clinical dissociation often seen in practice [19]. A patient may present with moderate CRP (moderate Axis 1) but dangerously high LDH (severe Axis 2). This dissociation is likely driven by "immunothrombosis" and microvascular emboli [35,36], a dysregulated interplay between inflammation and coagulation [36,37]. The strong correlation between LDH and D-dimer observed in our study (r = 0.395) supports this hypothesis that microvascular thrombosis exacerbates hypoxic tissue injury, releasing high levels of intracellular LDH due to cytoplasmic leakage [18] even when systemic inflammation is not proportionally elevated [38].

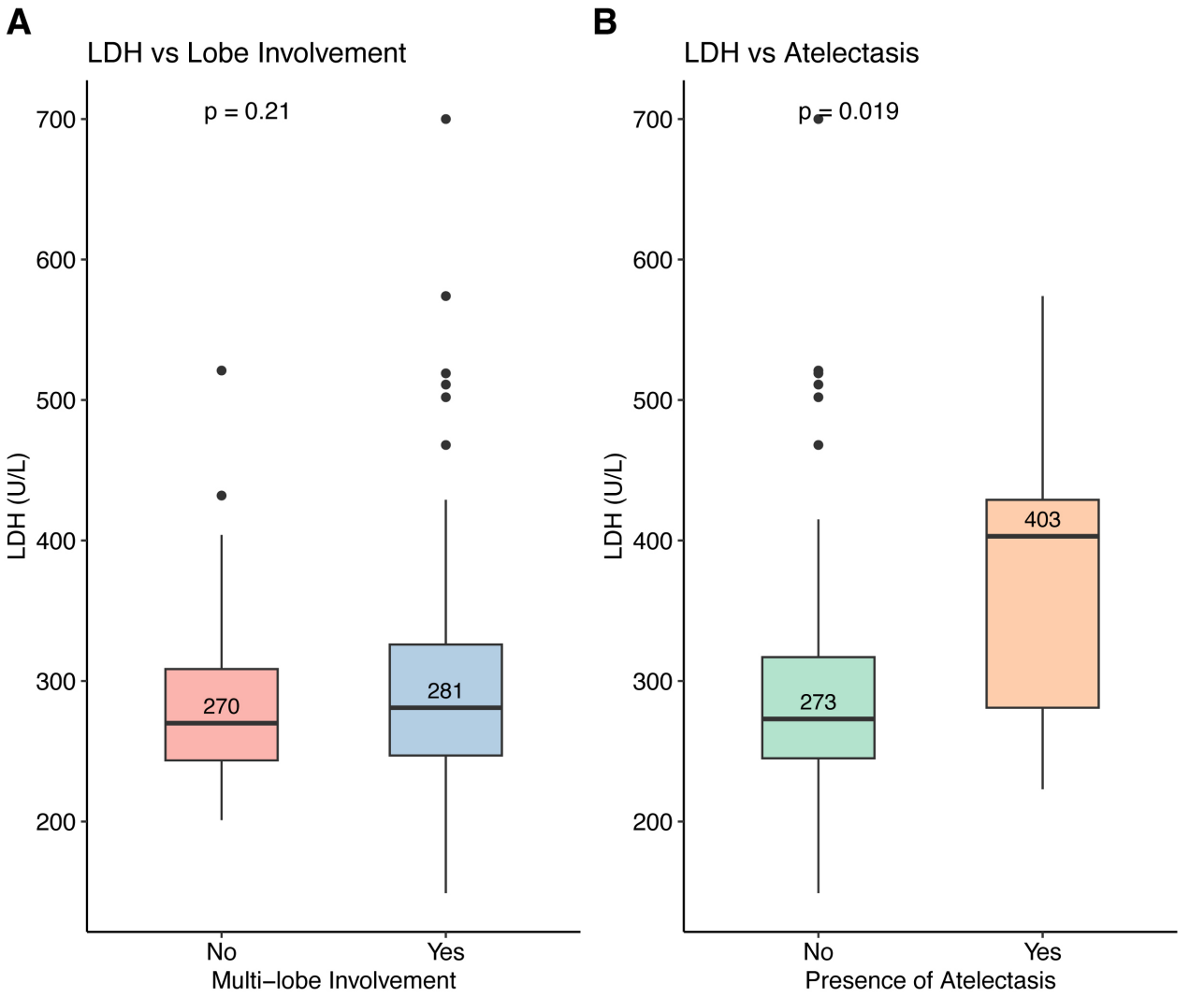

Fig. 6. Association between serum LDH levels and lung imaging phenotypes. Box plots displaying the difference in LDH levels stratified by radiological features. (A) Comparison between patients with single-lobe involvement versus those with multi-lobe/bilateral involvement. (B) Comparison between patients with and without pulmonary atelectasis. Elevated LDH levels are significantly associated with the presence of atelectasis but not with the extent of multi-lobe involvement, suggesting that LDH reflects local hypoxic tissue injury rather than the spatial burden of inflammation.

Therefore, our combined nomogram prevents the underestimation of risk in these silent hypoxic patients by capturing both the intensity of the immune attack and the severity of the resultant tissue injury.

It is important to note that while this study focused on SMPP as the primary outcome, RMPP represents a more severe and clinically distinct entity, defined by a lack of response to macrolide therapy for $\geq$7 days. The overlap between SMPP and RMPP is substantial but not complete, as not all severe cases progress to refractory disease. Our biomarker model was designed for early stratification of severity at the time of admission, which precedes and may predict the trajectory toward refractoriness. Prior studies have shown that LDH is particularly elevated in RMPP [19,20], consistent with our finding that LDH reflects tissue necrosis rather than systemic inflammation alone. Future studies should directly compare biomarker profiles between the SMPP-non-RMPP and SMPP-RMPP subgroups to refine the thresholds for escalating therapy.

Based on our ROC analysis, we propose the following reference thresholds for clinical risk stratification: LDH $>$291.50 U/L warrants heightened attention, particularly in the presence of atelectasis, while IL-6 $>$19.84 pg/mL suggests significant systemic immune activation consistent with an early cytokine storm. When both thresholds are exceeded simultaneously, clinicians should strongly consider early corticosteroid administration and serial bronchoscopic evaluation. These thresholds are derived from this single-center cohort and require prospective validation; they should be interpreted as complementary to, rather than a replacement for, comprehensive clinical assessment.

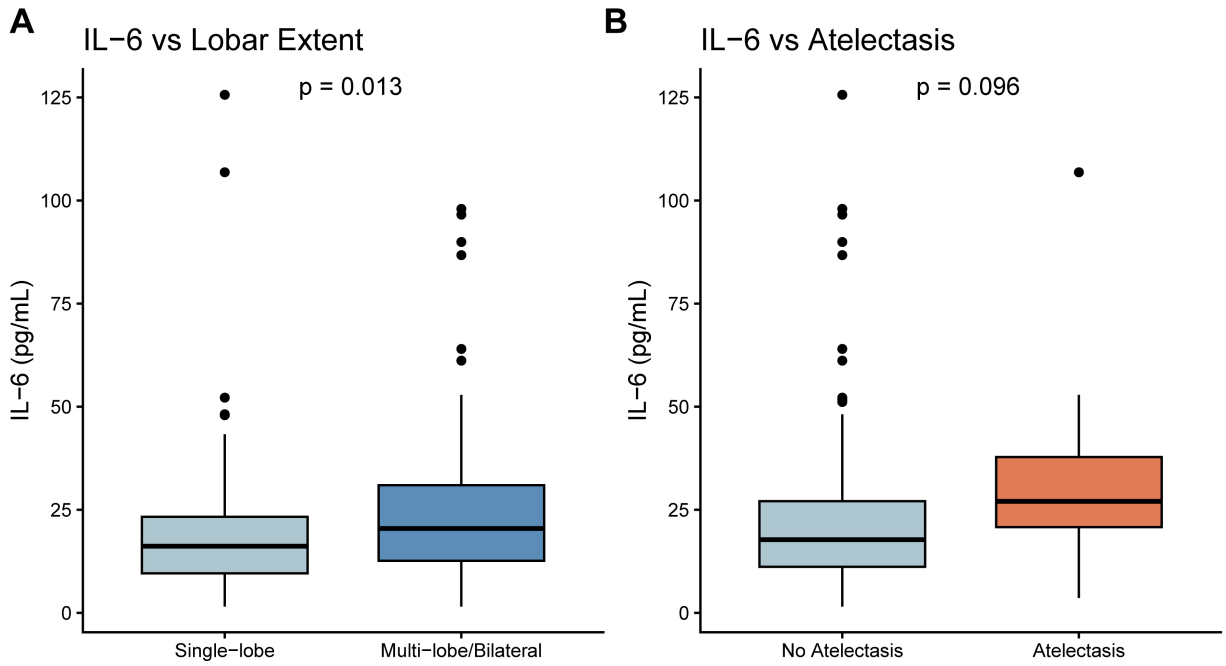

Fig. 7. Association between serum IL-6 levels and lung imaging phenotypes. Box plots displaying the difference in IL-6 levels stratified by radiological features. (A) Comparison between patients with single-lobe involvement versus those with multi-lobe/bilateral involvement. (B) Comparison between patients with and without pulmonary atelectasis.

The complementary nature of these two biomarkers underscores the value of the combined model. Relying solely on IL-6 may overlook cases where the systemic inflammatory response is moderate, but significant local tissue necrosis (high LDH) has already commenced. Conversely, relying only on LDH might delay the identification of patients in the early cytokine storm phase before significant cellular damage occurs. Our combined nomogram captures both the intensity of the immune attack (IL-6) and the severity of the resultant tissue injury (LDH). This dual-axis assessment explains why the combined model outperformed individual markers in terms of AUC.

Statistical significance does not always translate to clinical effectiveness; however, our use of Decision Curve Analysis (DCA) bridges this gap [39,40]. The DCA demonstrated that using the nomogram to guide treatment decisions provides a higher net benefit than "treat-all" or "treat-none" strategies across probability thresholds of 10% to 75%. This wide range is particularly relevant in pediatric practice, accommodating both risk-averse clinicians, who may intervene at lower probabilities, and those in resource-limited settings who require higher diagnostic certainty [39,40]. By strictly defining fever duration as the period prior to admission, the model avoids circular reasoning and ensures applicability at the time of initial clinical encounter, facilitating prompt triage [41].

The value of our nomogram extends beyond a simple probability score; it encourages clinicians to consider pathological dimensions. High IL-6 warrants aggressive immunomodulation (e.g., corticosteroids) to dampen the cytokine storm, whereas disproportionately high LDH—especially in the presence of atelectasis—should prompt vigilance for airway obstruction, necessitating consideration of airway clearance therapies or anticoagulation. This nuanced understanding transforms the biomarkers from simple high or low indicators into specific guides for targeted therapeutic intervention.

Despite these promising findings, several limitations warrant consideration. This study employed a single-center retrospective design, which may be susceptible to selection bias arising from the referral patterns, diagnostic practices, and patient demographics specific to our institution. Therefore, the generalizability of the nomogram to other centers requires caution. To mitigate this concern within the current dataset, we applied strict, guideline-based inclusion and exclusion criteria and confirmed the absence of significant demographic imbalances between groups. Nonetheless, prospective external validation in multi-center cohorts is essential before clinical implementation. Although we excluded co-infections, the potential influence of undetected viral pathogens cannot be entirely ruled out. Future studies should incorporate prospective designs with serial biomarker measurements. Particularly, the kinetic trajectories of LDH and IL-6 during treatment, and whether their rates of decline correlate with treatment response or risk of progression to refractory disease, remain unexamined in the current dataset and represent an important direction for investigation. Such longitudinal data would extend the clinical utility of these biomarkers from admission-based risk stratification to dynamic prognostic monitoring throughout

the disease course. It is noteworthy that clinical practice guidelines advocate heightened vigilance for SMPP from day 5 of persistent high fever, a threshold that precedes the $\geq$7-day formal grouping criterion applied in this study. Our biomarker-based nomogram is specifically designed to operate within this critical window, providing objective, quantifiable risk stratification during the period when clinical judgment alone is most challenged. Additionally, the absence of systematic seasonal distribution data in this study may limit the generalizability of our findings to specific epidemic periods of Mycoplasma pneumoniae infection. Furthermore, the mechanistic "two-axis" model proposed here is inferred from indirect clinical and biomarker evidence rather than direct histopathology. Because lung tissue biopsy is rarely feasible in pediatric SMPP, future studies employing bronchoalveolar lavage analysis or autopsy data in fatal cases would be valuable to validate this framework. Moreover, the classification of disease severity was performed by the clinical team responsible for patient care rather than by independent reviewers blinded to laboratory data, which introduces the risk of ascertainment bias. More prospective studies should incorporate independent, blinded adjudication of SMPP diagnosis to strengthen the validity of the grouping criteria. While internal validation was performed via bootstrap resampling (B = 1000), the absence of external validation in an independent cohort remains a limitation. The bootstrap-corrected calibration demonstrated good agreement (MAE = 0.061); however, the actual generalizability of the nomogram's calibration and discrimination can only be confirmed through prospective validation in geographically and institutionally distinct populations. Finally, the sensitivity of the combined model at the selected cut-off was 62.5%, reflecting a deliberate optimization toward high specificity (0.827) to minimize unnecessary escalation of treatment in non-severe patients. Clinicians are therefore advised to use the nomogram as a complementary risk stratification tool in conjunction with comprehensive clinical assessment, rather than as a standalone diagnostic instrument; the threshold probability may be adjusted according to the clinical context and institutional resources.

Conclusion

LDH and IL-6 reflect distinct but synergistic pathological processes in the progression of MPP. IL-6 characterizes the systemic inflammatory magnitude, while LDH serves as a marker for tissue hypoxia and complications such as atelectasis. The developed nomogram, validated to be effective even in the early phase of illness, provides a precise tool for stratifying high-risk children. By capturing the signals of cytokine storm and tissue hypoxia before the onset of persistent fever, this tool optimizes the timing for rational therapeutic decision-making.

Availability of Data and Materials

The data that support the findings of this study are available from the corresponding author upon reasonable request.

Author Contributions

RNZ and DKH designed the research study. RNZ and CQZ performed the research. JHL and DKH analyzed the data. DKH drafted the article. All authors contributed to important editorial changes in the manuscript. All authors read and approved the final manuscript. All authors have participated sufficiently in the work and agreed to be accountable for all aspects of the work.

Ethics Approval and Consent to Participate

The study protocol was conducted in accordance with the principles of the Declaration of Helsinki and was approved by the Ethics Committee of The Affiliated Yangming Hospital of Ningbo University (approval number: 2026-01-003), and the requirement for informed consent was waived due to the retrospective nature of the study.

Acknowledgment

Not applicable.

Funding

This research received no external funding.

Conflict of Interest

The authors declare no conflict of interest.

References

[1] Waites KB, Xiao L, Liu Y, Balish MF, Atkinson TP. Mycoplasma pneumoniae from the Respiratory Tract and Beyond. Clinical Microbiology Reviews. 2017; 30: 747–809. https://doi.org/10.1128/CMR.00114-16.

[2] Sharplin L, Goyal V. *Mycoplasma pneumoniae* respiratory tract infections in children: when and how to diagnose and treat. Breathe. 2025; 21: 250046. https://doi.org/10.1183/20734735.0046-2025.

[3] Meyer Sauteur PM, Beeton ML. Mycoplasma pneumoniae: delayed re-emergence after COVID-19 pandemic restrictions. The Lancet. Microbe. 2024; 5: e100–e101. https://doi.org/10.1016/S2666-5247(23)00344-0.

[4] You J, Zhang L, Chen W, Wu Q, Zhang D, Luo Z, *et al*. Epidemiological characteristics of mycoplasma pneumoniae in hospitalized children before, during, and after COVID-19 pandemic restrictions in Chongqing, China. Frontiers in Cellular and Infection Microbiology. 2024; 14: 1424554. https://doi.org/10.3389/fcimb.2024.1424554.

[5] Wang X, Li M, Luo M, Luo Q, Kang L, Xie H, *et al*. *Mycoplasma pneumoniae* triggers pneumonia epidemic in autumn and winter in Beijing: a multicentre, population-based epidemiological

study between 2015 and 2020. Emerging Microbes & Infections. 2022; 11: 1508–1517. https://doi.org/10.1080/22221751.2022.2078228.

[6] Kim EK, Youn YS, Rhim JW, Shin MS, Kang JH, Lee KY. Epidemiological comparison of three Mycoplasma pneumoniae pneumonia epidemics in a single hospital over 10 years. Korean Journal of Pediatrics. 2015; 58: 172–177. https://doi.org/10.3345/kjp.2015.58.5.172.

[7] Yang T, Lian H, Liao J, Zeng Y, Li J, Lin C, *et al*. Epidemiological characteristics and meteorological factors of acute respiratory infections (ARIs) in hospitalized children in eastern Guangdong, China. Scientific Reports. 2024; 14: 25518. https://doi.org/10.1038/s41598-024-77005-5.

[8] Yang S, Lu S, Guo Y, Luan W, Liu J, Wang L. A comparative study of general and severe mycoplasma pneumoniae pneumonia in children. BMC Infectious Diseases. 2024; 24: 449. https://doi.org/10.1186/s12879-024-09340-x.

[9] Liu J, He R, Zhang X, Zhao F, Liu L, Wang H, *et al*. Clinical features and "early" corticosteroid treatment outcome of pediatric *mycoplasma pneumoniae* pneumonia. Frontiers in Cellular and Infection Microbiology. 2023; 13: 1135228. https://doi.org/10.3389/fcimb.2023.1135228.

[10] Luo Z, Luo J, Liu E, Xu X, Liu Y, Zeng F, *et al*. Effects of prednisolone on refractory mycoplasma pneumoniae pneumonia in children. Pediatric Pulmonology. 2014; 49: 377–380. https://doi.org/10.1002/ppul.22752.

[11] Subspecialty Group of Respiratory, the Society of Pediatrics, Chinese Medical Association, China National Clinical Research Center of Respiratory Diseases, Editorial Board, Chinese Journal of Pediatrics. Evidence-based guideline for the diagnosis and treatment of *Mycoplasma pneumoniae* pneumonia in children (2023). Pediatric Investigation. 2025; 9: 1–11. https://doi.org/10.1002/ped4.12469.

[12] Tong L, Huang S, Zheng C, Zhang Y, Chen Z. Refractory *Mycoplasma pneumoniae* Pneumonia in Children: Early Recognition and Management. Journal of Clinical Medicine. 2022; 11: 2824. https://doi.org/10.3390/jcm11102824.

[13] Ding L, Jiang Y. Biomarkers associated with the diagnosis and prognosis of *Mycoplasma pneumoniae* pneumonia in children: a review. Frontiers in Cellular and Infection Microbiology. 2025; 15: 1552144. https://doi.org/10.3389/fcimb.2025.1552144.

[14] Huang X, Gu H, Wu R, Chen L, Lv T, Jiang X, *et al*. Chest imaging classification in Mycoplasma pneumoniae pneumonia is associated with its clinical features and outcomes. Respiratory Medicine. 2024; 221: 107480. https://doi.org/10.1016/j.rmed.2023.107480.

[15] Zhong H, Yin R, Zhao R, Jiang K, Sun C, Dong X. Analysis of Clinical Characteristics and Risk Factors of Plastic Bronchitis in Children With *Mycoplasma pneumoniae* Pneumonia. Frontiers in Pediatrics. 2021; 9: 735093. https://doi.org/10.3389/fped.2021.735093.

[16] Tian F, Chen LP, Yuan G, Zhang AM, Jiang Y, Li S. Differences of TNF-α, IL-6 and Gal-3 in lobar pneumonia and bronchial pneumonia caused by mycoplasma pneumoniae. Technology and Health Care. 2020; 28: 711–719. https://doi.org/10.3233/THC-192011.

[17] Hirano T. IL-6 in inflammation, autoimmunity and cancer. International Immunology. 2021; 33: 127–148. https://doi.org/10.1093/intimm/dxaa078.

[18] Wang LP, Hu ZH, Jiang JS, Jin J. Serum inflammatory markers in children with *Mycoplasma pneumoniae* pneumonia and their predictive value for mycoplasma severity. World Journal of Clinical Cases. 2024; 12: 4940–4946. https://doi.org/10.12998/wjcc.v12.i22.4940.

[19] Lee E, Choi I. Clinical Usefulness of Serum Lactate Dehydrogenase Levels in Mycoplasma pneumoniae Pneumonia in Children. Indian Journal of Pediatrics. 2022; 89: 1003–1009. https://doi.org/10.1007/s12098-022-04205-0.

[20] Inamura N, Miyashita N, Hasegawa S, Kato A, Fukuda Y, Saitoh A, *et al*. Management of refractory Mycoplasma pneumoniae pneumonia: utility of measuring serum lactate dehydrogenase level. Journal of Infection and Chemotherapy. 2014; 20: 270–273. https://doi.org/10.1016/j.jiac.2014.01.001.

[21] Mu SY, Zou YX, Guo YS, Huang B, Gao WW, Zhang T, *et al*. Clinical characteristics and predictive factors for plastic bronchitis in children with severe *Mycoplasma pneumoniae* pneumonia. Chinese Journal of Pediatrics. 2024; 62: 861–866. https://doi.org/10.3760/cma.j.cn112140-20240417-00272. (In Chinese)

[22] Keddie S, Ziff O, Chou MKL, Taylor RL, Heslegrave A, Garr E, *et al*. Laboratory biomarkers associated with COVID-19 severity and management. Clinical Immunology. 2020; 221: 108614. https://doi.org/10.1016/j.clim.2020.108614.

[23] Subspecialty Group of Respiratory Diseases, The Society of Pediatrics, Chinese Medical Association, Editorial Board, Chinese Journal of Pediatrics. Guidelines for management of community acquired pneumonia in children (the revised edition of 2013) (I). Chinese Journal of Pediatrics. 2013; 51: 745–752. (In Chinese)

[24] Subspecialty Group of Respiratory Diseases, The Society of Pediatrics, Chinese Medical Association The Editorial Board, Chinese Journal of Pediatrics. Guidelines for management of community acquired pneumonia in children(the revised edition of 2013) (II). Chinese Journal of Pediatrics. 2013; 51: 856–862. (In Chinese)

[25] Subspecialty Group of Respiratory, the Society of Pediatrics, Chinese Medical Association, Editorial Board, Chinese Journal of Pediatrics, China Medicine Education Association Committee on Pediatrics. Guidelines for the management of community-acquired pneumonia in children (2024 revision). Chinese Journal of Pediatrics. 2024; 62: 920–930. https://doi.org/10.3760/cma.j.cn112140-20240728-00523. (In Chinese)

[26] Wang H, Zhang Y, Zhao C, Peng Y, Song W, Xu W, *et al*. Serum IL-17A and IL-6 in paediatric *Mycoplasma pneumoniae* pneumonia: implications for different endotypes. Emerging Microbes & Infections. 2024; 13: 2324078. https://doi.org/10.1080/22221751.2024.2324078.

[27] Feng L, Mo J, Zhu J. Risk factors analysis of Mycoplasma pneumoniae infection in children and diagnostic value of IL-6 and STAT3. Medicine. 2025; 104: e44772. https://doi.org/10.1097/MD.0000000000044772.

[28] Pepys MB, Hirschfield GM. C-reactive protein: a critical update. The Journal of Clinical Investigation. 2003; 111: 1805–1812. https://doi.org/10.1172/JCI18921.

[29] Engler H, Brinkhoff A, Wilde B, Kribben A, Rohn H, Witzke O, *et al*. Endotoxin-Induced Physiological and Psychological Sickness Responses in Healthy Humans: Insights into the Post-Acute Phase. Neuroimmunomodulation. 2023; 30: 268–276. https://doi.org/10.1159/000534444.

[30] Klein R, Nagy O, Tóthová C, Chovanová F. Clinical and Diagnostic Significance of Lactate Dehydrogenase and Its Isoenzymes in Animals. Veterinary Medicine International. 2020; 2020: 5346483. https://doi.org/10.1155/2020/5346483.

[31] Zhang J, Wang T, Li R, Ji W, Yan Y, Sun Z, *et al*. Prediction of risk factors of bronchial mucus plugs in children with Mycoplasma pneumoniae pneumonia. BMC Infectious Diseases. 2021; 21: 67. https://doi.org/10.1186/s12879-021-05765-w.

[32] Yanhong R, Shuai Z, Dan C, Xiaomin S. Predictive value of lactate dehydrogenase for Mycoplasma pneumoniae necrotizing pneumonia in children based on decision curve analysis and dose-response analysis. Scientific Reports. 2024; 14: 9803. https://doi.org/10.1038/s41598-024-60359-1.

[33] Gupta GS. The Lactate and the Lactate Dehydrogenase in Inflammatory Diseases and Major Risk Factors in COVID-19 Pa-

tients. Inflammation. 2022; 45: 2091–2123. https://doi.org/10.1007/s10753-022-01680-7.

[34] Yang K, Holt M, Fan M, Lam V, Yang Y, Ha T, *et al*. Cardiovascular Dysfunction in COVID-19: Association Between Endothelial Cell Injury and Lactate. Frontiers in Immunology. 2022; 13: 868679. https://doi.org/10.3389/fimmu.2022.868679.

[35] Cheng R, Wang Q, Jiang L, Liu LM. Pulmonary thromboembolism due to Mycoplasma pneumoniae in children: a case report and literature review. BMC Pediatrics. 2024; 24: 816. https://doi.org/10.1186/s12887-024-05283-z.

[36] Zheng Y, Hua L, Zhao Q, Li M, Huang M, Zhou Y, *et al*. The Level of D-Dimer Is Positively Correlated With the Severity of *Mycoplasma pneumoniae* Pneumonia in Children. Frontiers in Cellular and Infection Microbiology. 2021; 11: 687391. https://doi.org/10.3389/fcimb.2021.687391.

[37] Engelmann B, Massberg S. Thrombosis as an intravascular effector of innate immunity. Nature Reviews. Immunology. 2013; 13: 34–45. https://doi.org/10.1038/nri3345.

[38] Frantzeskaki F, Armaganidis A, Orfanos SE. Immunothrombosis in Acute Respiratory Distress Syndrome: Cross Talks between Inflammation and Coagulation. Respiration. 2017; 93: 212–225. https://doi.org/10.1159/000453002.

[39] Vickers AJ, Elkin EB. Decision curve analysis: a novel method for evaluating prediction models. Medical Decision Making. 2006; 26: 565–574. https://doi.org/10.1177/0272989X06295361.

[40] Vickers AJ, Van Calster B, Steyerberg EW. Net benefit approaches to the evaluation of prediction models, molecular markers, and diagnostic tests. BMJ (Clinical Research Ed.). 2016; 352: i6. https://doi.org/10.1136/bmj.i6.

[41] Efthimiou O, Seo M, Chalkou K, Debray T, Egger M, Salanti G. Developing clinical prediction models: a step-by-step guide. BMJ (Clinical Research Ed.). 2024; 386: e078276. https://doi.org/10.1136/bmj-2023-078276.